



Planar liquid volume fraction measurements in air-blast sprays using SLIPI technique with numerical corrections

Aniket P. Kulkarni¹ · D. Deshmukh¹

Received: 13 April 2018 / Accepted: 22 August 2018 / Published online: 30 August 2018
© Springer-Verlag GmbH Germany, part of Springer Nature 2018

Abstract

A methodology to improve the accuracy of liquid volume fraction measurement in a dense spray is presented. A combination of experimental technique, structured laser illumination and planar imaging (SLIPI) and numerical corrections is used to overcome losses in conventional planar laser-induced fluorescence (PLIF) imaging. A quantitative distribution of liquid volume fraction in a plane is obtained using corrected SLIPI–PLIF signal and PDIA (particle/droplet imaging analysis) technique. The methodology is applied to air-blast sprays for GLRs (gas to liquid mass ratio) 1, 2.5 and 4. The effect of multiple scattering is significantly high in the conventional PLIF signal imaging. A hollow cone spray geometry is observed at a GLR of 1 using the improved imaging technique. An increase in GLR from 1 to 4 leads to uniform distribution of liquid in a spray plane. A significant contribution of multiple scattering ($\sim 62\%$) is observed in the conventional PLIF signal at GLR 4 along the axis of the spray. The symmetry in the SLIPI–PLIF signal is restored using the numerical corrections. The liquid volume fraction measurements from SLIPI–PLIF technique are further improved with the numerical corrections.

1 Introduction

Atomization of liquid governs process efficiency in many industrial applications. Distribution of liquid controls effectiveness of processes in spray coating, pharmaceutical applications, combustion devices, etc. [19]. Air–fuel mixture formation process, and hence emissions and combustion, are influenced by the liquid fuel distribution in a combustor [18, 33, 34]. Therefore, it is important to measure the distribution of liquid fuel (liquid volume fraction) in a spray.

Planar laser-induced fluorescence (PLIF) and laser beam extinction are commonly employed optical techniques for liquid volume fraction measurements in a spray [10, 12, 29]. Labs and Parker [17] measured liquid volume fraction in a diesel spray using extinction of infrared wavelength laser beam at various axial and radial locations. This is a point (probe volume diameter 0.15 mm) measurement technique and involves longer measurement times to get planar liquid volume fraction distribution. Liquid mass distribution in a spray plane can also be obtained using PLIF imaging [11].

However, various losses in PLIF signal measurement results in error in the liquid volume fraction measurements [11, 20, 27]. The scattering and the absorption of a laser sheet, due to droplet clouds in a spray, reduce the intensity of the incident laser sheet. This loss is termed as laser sheet extinction loss [6, 7, 20, 31]. The fluorescence signal, which travels from a laser sheet to a detector, is absorbed in liquid droplets due to overlapping of emission and absorption spectra of the fluorescence dye [4]. This loss is termed as auto-absorption of the fluorescence signal. The multiple scattering of a signal, also called as secondary emission, may be another important source of an error in laser sheet imaging [9, 13, 20]. Many attempts have been made to compensate these losses. Talley et al. [30] proposed a correction for laser extinction using counter-propagating laser sheets. Koh et al. [11] corrected signal attenuation using the geometric mean value of the intensities, obtained using two cameras. The loss in the fluorescence signal due to auto-absorption of the fluorescence signal and absorption of the laser sheet can be corrected using Beer–Lambert’s law [26]. Abu-Gharbieh et al. [1] proposed an approach to compensate a loss in a laser sheet due to scattering [26]. Overall, various correction methods have been proposed in the literature to correct losses due to laser extinction and signal attenuation in the PLIF signal.

Deshmukh and Ravikrishna [8] proposed a methodology to measure planar liquid volume fraction in dense sprays

✉ D. Deshmukh
dldeshmukh@iiti.ac.in

¹ Spray and Combustion Laboratory, Discipline of Mechanical Engineering, Indian Institute of Technology Indore, Indore, India

using PLIF and particle droplet imaging analysis (PDIA) techniques. Numerical corrections were used to compensate signal attenuation and laser extinction loss in the PLIF signals. However, the contribution of multiple scattering was neglected in this work. Labs and Parker [16] quantified errors from multiple-scattering effects for the infrared scattering in liquid volume fraction measurement at an ambient condition, high ambient pressure, and a combusting condition. Labs and Parker [16] reported a large error in measurement due to multiple scattering effects at the high ambient pressure and non-evaporative conditions due to higher optical depths at these conditions. Brown et al. [4] attempted to reduce multiple scattering by scanning the spray with a narrow laser beam, instead of a laser sheet, in a fan spray. They observed that the results were consistent with phase Doppler anemometry measurements. However, this method involves a long measurement time. A planar technique, structured laser illumination planar imaging (SLIPI) reduces the contribution of multiple scattering in a planar imaging [2, 3, 13, 14, 22]. The SLIPI technique reduces the effect of multiple scattering in Mie and PLIF imaging which can be used in dense sprays to get more accurate measurements of droplet diameter, spray structure, liquid volume fraction and temperature [3, 13, 22, 25]. A combination of SLIPI–PLIF and SLIPI–Mie is used to obtain drop sizing in a plane in a hollow cone spray [23]. Furthermore, SLIPI–PLIF is used to measure temperature of liquid using a combination of SLIPI and two-color PLIF [22, 25]. Mishra et al. [25] used SLIPI with two-color PLIF to measure water temperature in the range of 25–85 °C in cuvette and in hollow cone spray. They reported improvements in sensitivity of the temperature measurements and more pronounced temperature gradients within the spray. Air entrainment and local equivalence ratio measurements are carried out using SLIPI–PLIF technique in a heavy-duty, optical diesel engine. It was observed that conventional PLIF measurements overestimate local equivalence ratio due to contribution of multiple scattering [5, 28]. However, SLIPI signals require corrections for laser extinction and signal attenuation using the numerical models for reliable measurements. Planar imaging techniques are preferred in literature since they provide planar distribution. Various losses in laser sheet and signal poses difficulty in using quantitative information from these techniques. It is necessary to improve these methods to get more accurate measurements.

In this work, the combination of SLIPI and numerical correction models is used to reduce contribution of multiple scattering and other errors in the PLIF imaging. A methodology to develop a Ronchi grating for high energy density laser is given. The liquid volume fraction measurements with SLIPI–PLIF signal are improved with the numerical corrections. The modified methodology is applied to air-blast sprays which are extensively used in stationary combustion

devices. Liquid volume fraction from SLIPI–PLIF technique with numerical corrections is compared with that from PDIA technique at various radial locations. Planar liquid volume fraction from SLIPI–PLIF signal with numerical correction is obtained at GLRs 1, 2.5 and, 4 in the air-blast sprays.

2 Experimental setup

The experimental setup consists of an air-blast spray rig and optical arrangements for PDIA technique and SLIPI experiments to capture Mie and PLIF signals (Fig. 1).

An optical arrangement consists of an Nd: YAG pulsed laser ($\lambda = 532$ nm, 200 mJ max. energy, 10 ns pulse width) as an illumination source. A combination of spherical and cylindrical lenses is used to generate a laser sheet of 60 mm height and thickness ~ 1 mm. Mie and PLIF signals are captured using a CCD camera (PCO Sensicam) and a macro lens. The field of view of the camera including imaging lens is 88 mm \times 60 mm in Mie and PLIF imaging with a pixel resolution of 88.5 μm per pixel. PLIF signal is acquired using a bandpass filter (centered at 560 nm, 32 nm FWHM) and a fluorescent dye (Rhodamine 6G with the concentration of 20 mg/L in water).

A Ronchi grating is an important element in the SLIPI experiments. Commercially available Ronchi gratings are damaged due to a high energy density of pulsed laser beam. A Ronchi grating (5 lp/mm) is developed using a sputtered thin film coating (thickness 500 nm) of aluminum on a glass slide. A mask is developed using a UV lithography. A wet etchant of acetic acid, phosphoric acid, and nitric acid is used for etching at room temperature (27 °C) for 3 min [32]. The developed Ronchi grating is able to withstand the high energy input of the laser beam. A frequency cutter is used to minimize unwanted residual line structure in the final SLIPI image. The Ronchi grating is moved in a vertical direction using a translational stage (5 μm resolution) to achieve spatial modulation of the structured laser sheet.

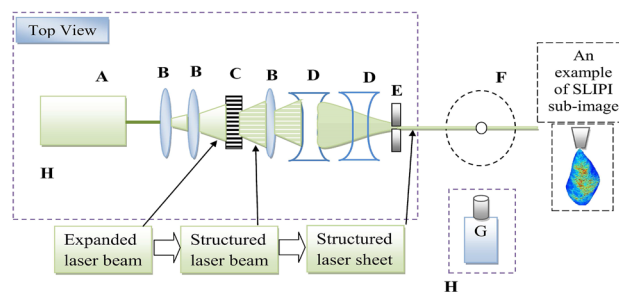


Fig. 1 An optical arrangement for SLIPI measurements. A Nd: YAG Laser, B spherical convex lens, C Ronchi grating with translation stage, D cylindrical lens, E frequency cutter, F air-blast spray, G CCD camera with macro lens and optical filter, H optical table

The experimental setup for the PDIA technique consists of a long-distance microscope coupled with a CCD camera to obtain a field of view of $1.92 \text{ mm} \times 1.44 \text{ mm}$. The liquid volume fraction at a point is determined with PDIA technique at respective operating conditions using depth of field of the optical setup [15]. An uncertainty in liquid volume fraction measurement in the PDIA technique is estimated as 24%. A commercially available externally mixed Delavan air-blast atomizer (30609-2) is used to generate an air-blast spray. The experiments are performed under non-evaporative ambient conditions. The water flow rate is kept constant (12 mL/min), and air flow rate is varied to get GLRs (gas to liquid mass ratio) 1, 2.5 and 4.

3 Methodology

The loss in the PLIF signal, due to scattering and absorption of the laser sheet, absorption of the fluorescence signal, and multiple scattering, is compensated with experimental and numerical corrections. The methodology for experimental and numerical corrections is given below.

- A spatially modulated laser sheet is used in the SLIPI technique to reduce multiple scattering in PLIF and Mie signals. The spatial modulation of the structured laser sheet is obtained by moving the Ronchi grating in the vertical direction using a translational stage. Three spatially modulated sub-images (I_1 , I_2 and I_3) are acquired at the period of one-third of the modulation. The SLIPI image is calculated using modulated images with Eq. 1. A conventional image (I_C) is obtained using Eq. 2. Various corrections, such as offset correction, mean intensity correction, and field-dependent correction, are applied on a SLIPI image to reduce residual line structure in a SLIPI image [13, 24]. Final SLIPI images for PLIF (SLIPI-PLIF) and Mie (SLIPI-Mie) are obtained by averaging 150 SLIPI images.

$$I_{\text{SLIPI}} = \frac{\sqrt{2}}{3} \cdot [(I_1 - I_2)^2 + (I_2 - I_3)^2 + (I_3 - I_1)^2]^{1/2} \quad (1)$$

and

$$I_C = \frac{I_1 + I_2 + I_3}{3}. \quad (2)$$

The averaged SLIPI images are then corrected for various losses with numerical corrections.

- The energy of the laser sheet reduces due to scattering while passing through the spray of high droplet number density. This loss in incident laser sheet leads to an error in SLIPI-PLIF signal. The scattering loss can be corrected using correction matrix ($CM_{\text{Mie}}(x, y)$) as proposed

by Abu-Gharbieh et al. [1]. The corrected signal is given by:

$$S_{(x,y)}^{\text{new}} = S_{(x,y)}^{\text{old}} \cdot CM_{\text{Mie}}(x, y) \quad (3)$$

$$\text{where } CM_{\text{Mie}}(x, y) = \exp \left(K \cdot \sum_{y=0}^{y=y-1} S_{(x,y)}^{\text{new}} \right)$$

where $S_{(x,y)}^{\text{old}}$ is the observed pixel intensity in the SLIPI-Mie image, $S_{(x,y)}^{\text{new}}$ is the compensated value for that pixel and K is an unknown constant. x is the distance from the nozzle tip along the axis of the spray and y is the radial distance in the direction of laser sheet. The unknown constant K is selected such that both sides of the spray image become symmetric about the spray axis assuming the spray is symmetric. The correction matrix (CM_{Mie}) is used to correct SLIPI-PLIF signal for the loss due to scattering of the laser sheet, using Eq. 4.

$$PLIF_{\text{corr,scattering}}(x, y) = PLIF(x, y) \times CM_{\text{Mie}}(x, y) \quad (4)$$

- The fluorescence signal is proportional to the volume of the liquid (V_F) present in the total pixel volume (V_T) [8, 26]. This is defined in terms of equivalent density (ρ_e) as given in Eq. 5:

$$\rho_e = \rho \cdot \frac{V_F}{V_T}. \quad (5)$$

Thus, the fluorescence signal in terms of ρ_e is given as:

$$S_F(x, y) = K_1 \cdot \rho_e(x, y). \quad (6)$$

The constant K_1 in the Eq. 6 is determined using the PDIA technique by calculating the total volume of droplets present in the measurement volume, i.e., liquid volume fraction at a point.

- The absorption of the fluorescence signal in the spray due to overlapping of emission and absorption spectra of the dye is corrected using Beer-Lambert's law. Similarly, the loss in the incident intensity of the laser sheet due to absorption in the spray is corrected separately. The combined equation for laser sheet scattering and absorption correction and auto-absorption correction of the PLIF signal is given by:

$$PLIF_{\text{corr}}(x, y) = SLIPI-PLIF(x, y) \cdot CM_{\text{Mie}}(x, y) \cdot \exp \left(\int_{y=0}^{y=L} \alpha \cdot \rho_e(x, y) \cdot dy \right) \cdot \exp \left(\int_{z=0}^{z=t} \alpha_{\text{auto}} \cdot \rho_e(x, z) \cdot dz \right) \quad (7)$$

where α is absorption coefficient ($1.5830 \text{ m}^2/\text{kg}$) and α_{auto} is auto-absorption coefficient ($0.7352 \text{ m}^2/\text{kg}$) for the dye and t is the liquid column present between the detector and the laser sheet (m), i.e., in z direction. The values of L and t are calculated as a distance from the spray edge to a pixel (x, y) in a binary PLIF image assuming the spray symmetry. The values for α and α_{auto} are obtained using a cuvette experiment and Beer–Lambert law for a known concentration of the dye. Equations 5 and 7 are solved simultaneously and iteratively to obtain $\rho_e(x, y)$ and $\text{PLIFcorr}(x, y)$. Equation 5 is then used to determine liquid volume fraction in a plane. More information on the numerical corrections can be found in the references [1, 8, 26].

A detailed methodology to obtain planar liquid volume fraction in a spray using SLIPI–PLIF technique and PDIA technique along with numerical corrections is explained in a flowchart given in Fig. 2.

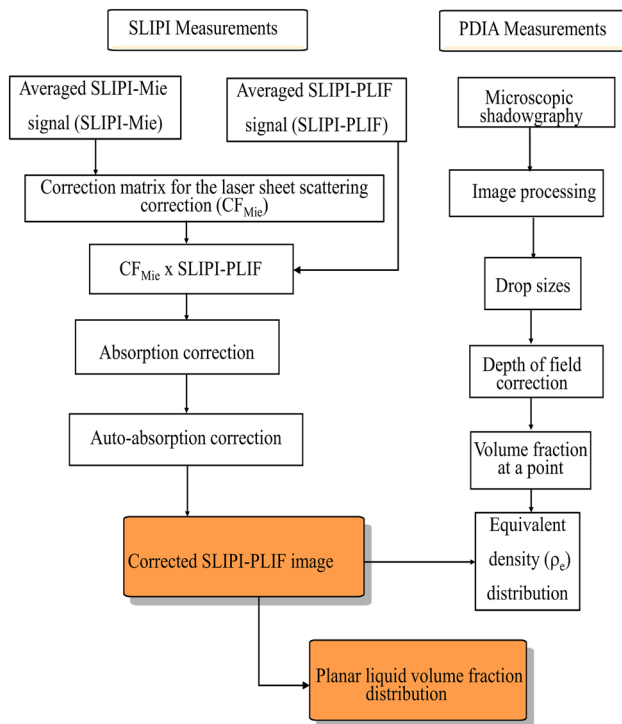


Fig. 2 A detailed methodology to obtain planar liquid volume fraction in a spray using SLIPI–PLIF technique and PDIA technique along with numerical corrections

4 Result and discussion

PLIF and Mie images are obtained using conventional and SLIPI techniques. These images are further corrected for losses. The improvement in the signals is compared in the following section.

4.1 Influence of corrections on the SLIPI–PLIF signal

Figure 3 compares PLIF signal from conventional and SLIPI–PLIF imaging at 30 mm below the nozzle tip for GLR 4. The laser sheet enters the spray from the left side. The conventional PLIF signal is higher than SLIPI signal at most of the locations. The difference in the PLIF signals may be attributed to the contribution of the multiple scattering due to high optical depth. The difference is significantly higher (around 62%) along the spray axis. This confirms that the contribution of the multiple scattering in the conventional PLIF signal can not be neglected.

Both the PLIF signals, conventional and SLIPI, are observed to be asymmetric about the spray axis. This asymmetry can be attributed to the laser sheet extinction. The symmetry is restored using the laser sheet absorption and the laser sheet scattering corrections. It is observed that contribution of laser sheet scattering correction is higher compared to that of absorption and auto-absorption corrections. A large number of small droplets are generated due to better atomization at this GLR condition. Hence, due to low liquid volume fraction, the contribution of absorption and auto-absorption corrections might be lower. Similarly, due to high droplet number density, the contribution of the laser sheet scattering correction might be higher. The observations are

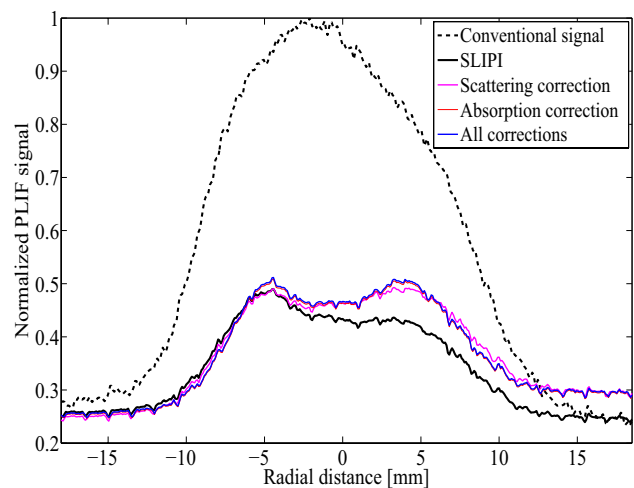
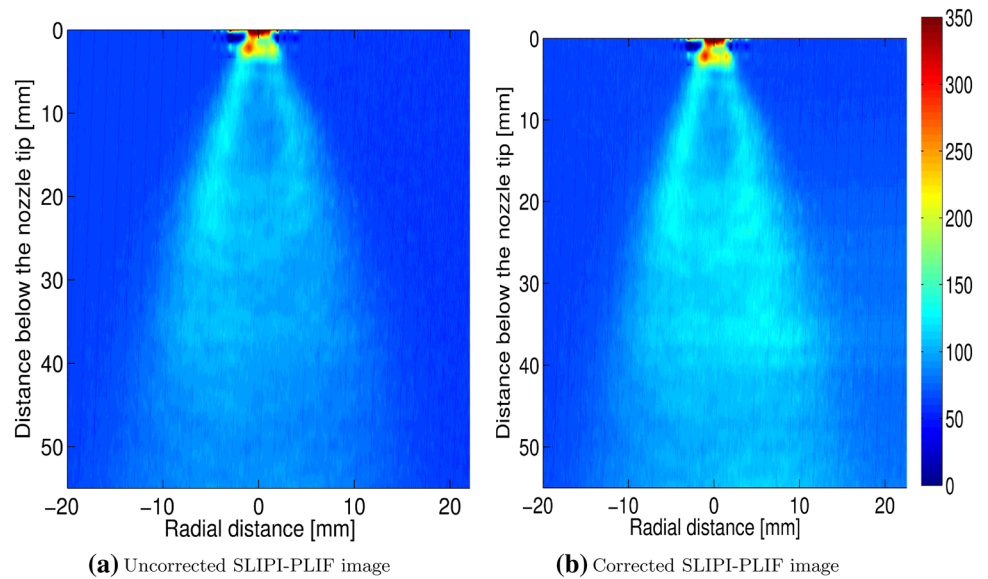


Fig. 3 Conventional and SLIPI–PLIF signals with numerical corrections at 30 mm below the nozzle tip for GLR 4. The laser sheet travels from left to right

further confirmed in Fig. 4 where the SLIPI–PLIF image at GLR 4, before and after numerical correction, are compared. Numerical corrections have improved the symmetry of the SLIPI–PLIF signal. In the uncorrected SLIPI–PLIF signal, the right half of the spray shows a lower signal intensity. The symmetry in the PLIF signal intensity about spray axis is restored in the corrected SLIPI–PLIF image.

Fig. 4 SLIPI–PLIF images before and after the numerical corrections for GLR 4. The laser sheet travels from left to right



4.2 Comparison of liquid volume fraction profiles from conventional and SLIPI–PLIF technique

The liquid volume fraction in the axial plane is obtained and compared for GLRs 1, 2.5 and, 4 using the PDIA technique. The numerical corrections are applied to improve the accuracy of the measurements.

Figure 5 compares liquid volume fraction profiles from conventional and SLIPI–PLIF techniques at 30 mm below the nozzle tip for GLR 4. The liquid volume fraction from SLIPI–PLIF is slightly lower than that from conventional PLIF. This lower liquid volume fraction from the

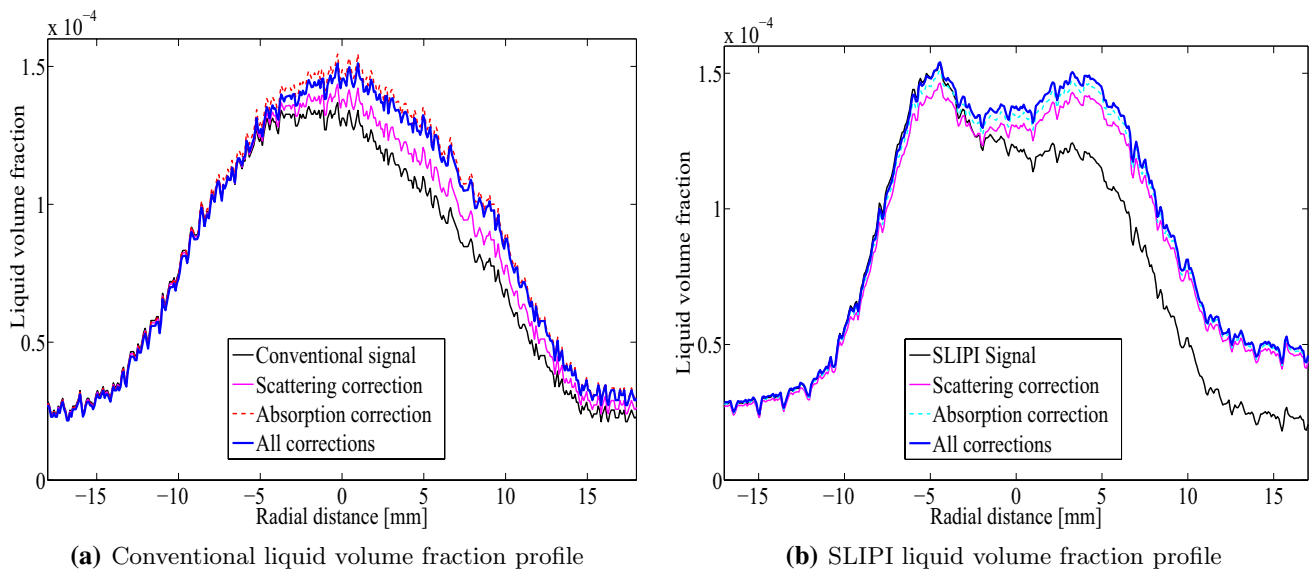


Fig. 5 A comparison of conventional and SLIPI liquid volume fraction profiles at 30 mm below the nozzle tip for GLR 4. The laser sheet travels from left to right

SLIPI–PLIF technique may be attributed to the reduction in the multiple scattering in the PLIF signal due to the SLIPI technique. The major difference in the liquid fraction profile is observed along the spray axis, where SLIPI–PLIF technique showed a bimodal distribution of the liquid volume fraction (Fig. 5b) compared to that of bell-shaped distribution from the conventional PLIF technique (Fig. 5a). A bell-shaped distribution shows that most of the liquid is accumulated along the spray axis, and hence a solid cone spray. On the other hand, a bimodal distribution indicates accumulation of the liquid around the edges of the spray. This implies a semi-solid cone spray at this axial distance.

The bimodal distribution of liquid is further confirmed at GLR 1 condition. Figure 6 shows a comparison of liquid volume fraction distributions from conventional and SLIPI–PLIF technique at GLR 1. The spray is observed to be a hollow cone spray from SLIPI–PLIF imaging (Fig. 6b). The liquid volume fraction distribution from conventional PLIF showed a solid cone spray (Fig. 6a). To further confirm this finding, the liquid volume fraction profiles obtained from SLIPI–PLIF and conventional PLIF are compared with PDIA measurements at various radial locations for GLR 1 (Fig. 7). Liquid volume fraction measurements from conventional and SLIPI–PLIF technique are in good agreement with that from PDIA measurements at spray periphery. However, a significant deviation is observed between liquid volume fraction from conventional PLIF imaging and that from PDIA technique along the spray axis. A contribution of multiple scattering in the conventional PLIF signal might have led to this disagreement. The liquid volume fraction measurements from SLIPI–PLIF technique are in good agreement with that from PDIA technique along the spray

Fig. 6 A comparison of conventional and SLIPI liquid volume fraction distributions for GLR 1

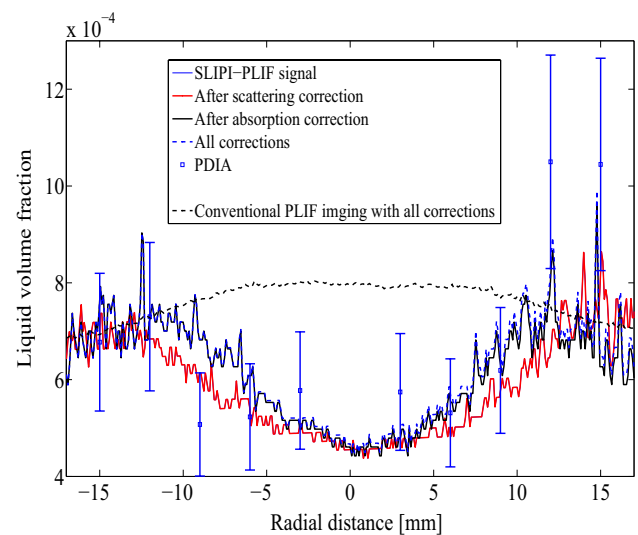
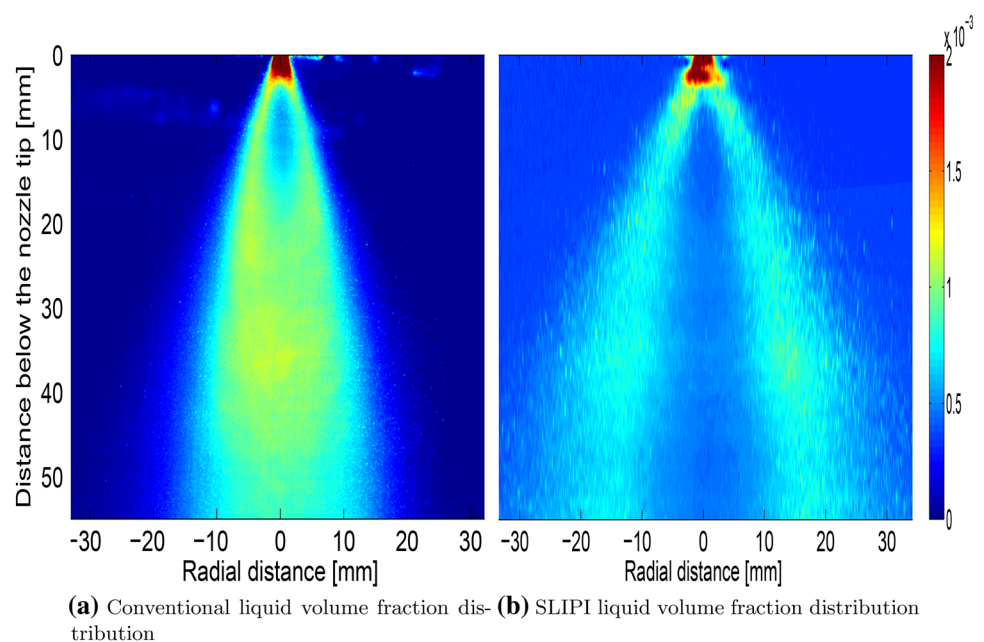


Fig. 7 A comparison of liquid volume fraction profiles from conventional and SLIPI–PLIF with various numerical corrections with liquid volume fraction from PDIA for GLR 1 at 30 mm below the nozzle tip

axis. This confirms that contribution of multiple scattering is reduced in the SLIPI–PLIF imaging.

Figure 7 compares the contribution of the numerical corrections in liquid fraction measurements using SLIPI–PLIF signal. The contribution of scattering correction is minimal due to low droplet number density at GLR 1. Large droplets are generated due to the poor atomization of the liquid at GLR 1. Hence, droplet number density might be low which might have reduced the contribution of the laser sheet scattering correction at GLR 1. The auto-absorption correction showed a marginal improvement. The contribution

of absorption of the laser sheet correction is high due to high liquid volume fraction which might absorb energy in the incident laser sheet. The maximum improvement in the liquid volume fraction measurement with all numerical corrections (around 18%) is observed at the spray periphery for GLR 1.

4.3 Radial liquid volume fraction profiles at various axial locations

Figure 8 compares the radial liquid volume fractions distribution at 20 mm, 30 mm, 40 mm and 50 mm below the nozzle tip for GLR 1 and 4. The liquid volume fraction profiles at GLR 1 shows that most of the liquid is accumulated along the spray periphery. This suggests a hollow cone spray structure at this GLR condition. At higher GLR condition (GLR 4), two distinct liquid volume fraction profiles are observed. The profiles at 20 mm and 30 mm below the nozzle tip shows bimodal distribution, whereas bell-shaped profiles are observed at 40 and 50 mm axial locations. This variation in radial liquid volume fraction profiles suggests a semi-solid cone spray at GLR 4. The transition of the spray from hollow cone spray to semi-solid cone spray with an increase in GLR may be attributed to an increase in axial velocity of the atomizing gas. The increased momentum of gas might have promoted uniform liquid distribution [21].

4.4 Planar liquid volume fraction at GLRs 1, 2.5 and 4

The liquid volume fraction distribution at GLRs 1, 2.5 and, 4 is compared in Fig. 9. GLR 1 shows significantly higher liquid volume fraction (max. 2×10^{-3}) along the spray edges.

This gives a hollow cone spray geometry at lower GLR. The swirling liquid with lower kinetic energy in the atomizing gas might have caused poor atomization of the liquid and larger droplets spread around the spray edges. Moreover, the liquid is spread non-uniformly at this GLR condition. When GLR is increased to 2.5 (Fig 9b), the liquid volume fraction decreased considerably (max. 1×10^{-3}). This can be attributed to an improved atomization due to an increase in kinetic energy of the atomizing air. However, the liquid is distributed unevenly in the spray plane, which may lead to a rich and lean pockets of the fuel–air mixture in a combustion chamber. At GLR 4 (Fig. 9c), low liquid fraction (max. 3.5×10^{-4}) is observed. The liquid is distributed uniformly which may further result in better combustion efficiency and lower emissions from a combustion device.

5 Conclusion

A methodology is proposed to improve the accuracy of liquid volume fraction measurement in a spray using combination of experimental and numerical tools. Liquid volume fraction distribution in a plane of an air-blast spray is measured using the SLIPI–PLIF technique. The SLIPI technique is used to reduce the error in the conventional PLIF signal due to multiple scattering. The errors due to laser sheet scattering, absorption of the laser sheet and auto-absorption in the SLIPI–PLIF signal are corrected using the numerical model. The contribution of multiple scattering is significant ($\sim 62\%$ for GLR 4, at 30 mm below the nozzle tip along the spray axis) in the conventional PLIF signal and hence cannot be neglected in the measurements. The symmetry in the SLIPI–PLIF signal intensity about spray axis is restored in

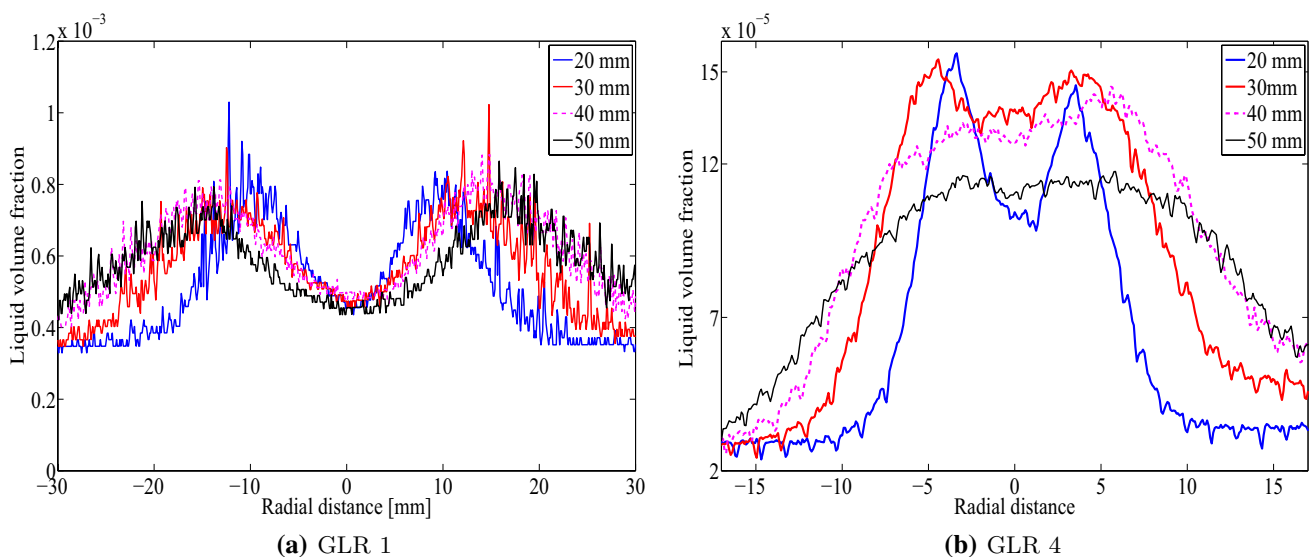


Fig. 8 Radial liquid volume fraction profiles at various axial locations for GLR 1 and GLR 4

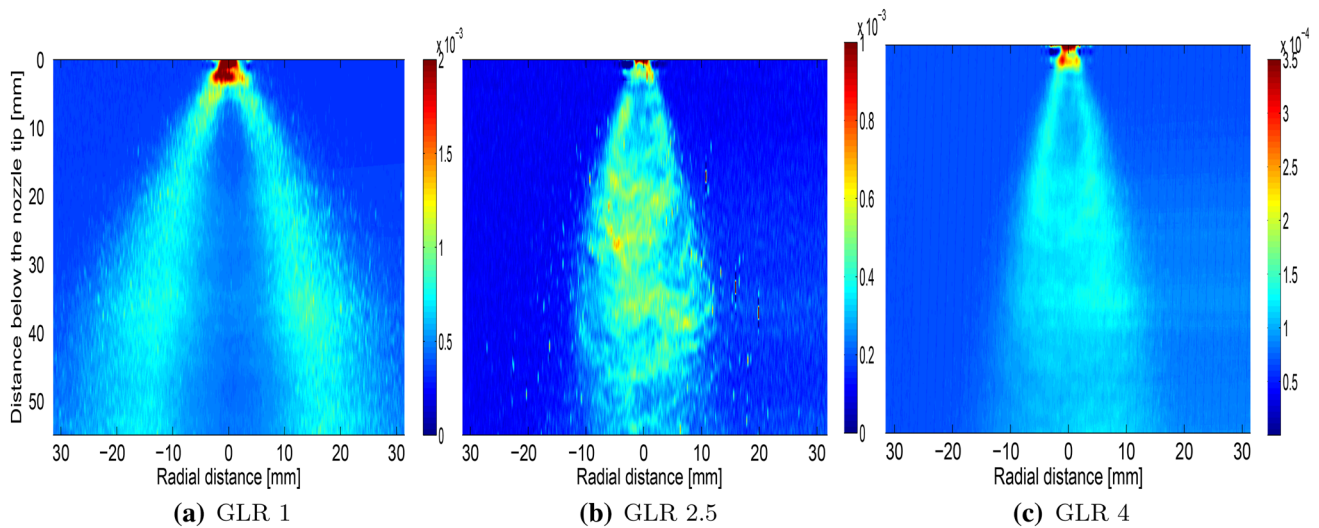


Fig. 9 Planar liquid volume fraction distribution at GLRs 1, 2.5 and 4 using SLIPI-PLIF technique

the corrected SLIPI-PLIF image using the numerical corrections. The improvement in the liquid volume fraction measurements is around 18% at spray periphery for GLR 1. The spray geometries from conventional PLIF showed a solid cone spray, whereas a hollow cone spray is observed from SLIPI-PLIF images at GLR 1 condition. The hollow cone geometry is further confirmed by comparing the liquid volume fraction measurements from PDIA technique. A good agreement is observed between SLIPI-PLIF and PDIA liquid volume fraction measurements. The modified methodology is used to measure planar liquid volume fraction in the air-blast sprays at GLR 1, 2.5 and 4. High liquid volume fraction with unevenly distributed liquid is observed at GLR 1 and 2.5. A uniformly distributed liquid is observed at GLR 4 due to improved atomization. The results show that presence of multiple scattering in conventional PLIF imaging cannot be neglected when these are used for quantitative or qualitative analysis.

Funding Funding was provided by SERB-DST India (Grant no. SB/S3/MMER/0028/2013).

References

1. R. Abu-Gharbieh, J.L. Persson, M. Försth, A. Rosén, A. Karlström, T. Gustavsson, Compensation method for attenuated planar laser images of optically dense sprays. *Appl. Opt.* **39**(8), 1260–1267 (2000)
2. E. Berrocal, E. Kristensson, P. Hottenbach, M. Aldén, G. Grünefeld, Quantitative imaging of a non-combusting diesel spray using structured laser illumination planar imaging. *Appl. Phys. B* **109**(4), 683–694 (2012)
3. E. Berrocal, E. Kristensson, M. Richter, M. Linne, M. Aldén, Application of structured illumination for multiple scattering suppression in planar laser imaging of dense sprays. *Opt. Express* **16**(22), 17870–17881 (2008)
4. C.T. Brown, V.G. McDonnell, D.G. Talley, Accounting for laser extinction, signal attenuation, and secondary emission while performing optical patterning in a single plane. In *Fifteenth Annual Conference on Liquid Atomization and Spray Systems, Madison, WI, USA* (2002)
5. C. Chartier, J. Sjöholm, E. Kristensson, O. Andersson, M. Richter, B. Johansson, M. Aldén, Air-entrainment in wall-jets using SLIPI in a heavy-duty diesel engine. *SAE Int. J. Engines* **5**, 1684–1692 (2012). <https://doi.org/10.4271/2012-01-1718>
6. A. Coghe, G.E. Cossali, Quantitative optical techniques for dense sprays investigation: a survey. *Opt. Lasers Eng.* **50**(1), 46–56 (2012)
7. C.S. Cooper, N.M. Laurendeau, Comparison of laser-induced and planar laser-induced fluorescence measurements of nitric oxide in a high-pressure, swirl-stabilized, spray flame. *Appl. Phys. B* **70**(6), 903–910 (2000)
8. D. Deshmukh, R.V. Ravikrishna, A method for measurement of planar liquid volume fraction in dense sprays. *Exp. Therm. Fluid Sci.* **46**, 254–258 (2013)
9. T.D. Fansler, S.E. Parrish, Spray measurement technology. A review. *Meas. Sci. Technol.* **26**(1), 012002 (2014)
10. R.K. Hanson, J.M. Seitzman, P.H. Paul, Planar laser-fluorescence imaging of combustion gases. *Appl. Phys. B* **50**(6), 441–454 (1990)
11. H. Koh, J. Jeon, D. Kim, Y. Yoon, J.-Y. Koo, Analysis of signal attenuation for quantification of a planar imaging technique. *Meas. Sci. Technol.* **14**(10), 18–29 (2003)
12. K. Kohse-Höinghaus, Quantitative laser-induced fluorescence: some recent developments in combustion diagnostics. *Appl. Phys. B* **50**(6), 455–461 (1990)
13. E. Kristensson, Structured Laser illumination planar imaging: SLIPI applications for spray diagnostics. Ph.D. Thesis, Lund University, Lund, 2012
14. E. Kristensson, L. Araneo, E. Berrocal, J. Manin, M. Richter, M. Aldén, M. Linne, Analysis of multiple scattering suppression using structured laser illumination planar imaging in scattering and fluorescing media. *Opt. Express* **19**(14), 13647–13663 (2011)

15. A.P. Kulkarni, D. Deshmukh, Spatial drop-sizing in airblast atomization—an experimental study. *At. Sprays* **27**(11), 949–961 (2017)
16. J. Labs, T. Parker, Multiple-scattering effects on infrared scattering measurements used to characterize droplet size and volume fraction distributions in diesel sprays. *Appl. Opt.* **44**(28), 6049–6057 (2005)
17. J. Labs, T. Parker, Two-dimensional droplet size and volume fraction distributions from the near-injector region of high-pressure diesel sprays. *At. Sprays* **16**, 843–855 (2006)
18. A.H. Lefebvre, Airblast atomization. *Prog. Energy Combust. Sci.* **6**(3), 233–261 (1980)
19. A. Lefebvre, *Atomization and Sprays* (CRC Press, Boca Raton, 1988)
20. M. Linne, Imaging in the optically dense regions of a spray: a review of developing techniques. *Prog. Energy Combust. Sci.* **39**(5), 403–440 (2013)
21. C. Liu, F. Liu, Y. Mao, M. Yong, X. Gang, Experimental investigation of performance of an air blast atomizer by planar laser sheet imaging technique. *J. Eng. Gas Turbines Power* **136**(2), 021601 (2014)
22. Y.N. Mishra, Droplet size, concentration, and temperature mapping in sprays using SLIPI-based techniques, Ph.D. Thesis, Lund University, Lund (2018)
23. Y.N. Mishra, E. Kristensson, E. Berrocal, Reliable LIF/Mie droplet sizing in sprays using structured laser illumination planar imaging. *Opt. Express* **22**(4), 4480–4492 (2014)
24. Y.N. Mishra, E. Kristensson, M. Koegl, J. Jönsson, L. Zigan, E. Berrocal, Comparison between two-phase and one-phase SLIPI for instantaneous imaging of transient sprays. *Exp. Fluids* **58**(9), 110 (2017)
25. Y.N. Mishra, F.A. Nada, S. Polster, E. Kristensson, E. Berrocal, Thermometry in aqueous solutions and sprays using two-color LIF and structured illumination. *Opt. Express* **24**(5), 4949–4963 (2016)
26. J.V. Pastor, J.J. Lopez, J.E. Juliá, J.V. Benajes, Planar laser-induced fluorescence fuel concentration measurements in isothermal diesel sprays. *Opt. Express* **10**(7), 309–323 (2002)
27. V. Sick, B. Stojkovic, Attenuation effects on imaging diagnostics of hollow-cone sprays. *Appl. Opt.* **40**(15), 2435–2442 (2001)
28. J. Sjöholm, C. Chartier, E. Kristensson, E. Berrocal, Y. Gallo, M. Richter, Ö. Andersson, M. Aldén, B. Johansson, Quantitative in-cylinder fuel measurements in a heavy duty diesel engine using structured laser illumination planar imaging (SLIPI). In *COMODIA 2012, MD2*, vol 3 (2012)
29. B.D. Stojkovic, V. Sick, Evolution and impingement of an automotive fuel spray investigated with simultaneous Mie/LIF techniques. *Appl. Phys. B* **73**(1), 75–83 (2001)
30. D. Talley, J. Verdieck, S. Lee, V. McDonnell, G. Samuelsen, Accounting for laser sheet extinction in applying PLLIF to sprays. In *34th Aerospace Sciences Meeting and Exhibit*, p. 469 (1996). <https://doi.org/10.2514/6.1996-469>
31. K. Verbeizen, R.J.H. Klein-Douwel, A.P. Van Vliet, A.J. Donkerbroek, W.L. Meerts, N.J. Dam, J.J. Ter Meulen, Attenuation corrections for in-cylinder no lif measurements in a heavy-duty diesel engine. *Appl. Phys. B* **83**(1), 155–166 (2006)
32. P. Walker, W.H. Tarn, *CRC Handbook of Metal Etchants* (CRC Press, Boca Raton, 1990)
33. F. Xing, A. Kumar, Y. Huang, S. Chan, C. Ruan, S. Gu, X. Fan, Flameless combustion with liquid fuel: a review focusing on fundamentals and gas turbine application. *Appl. Energy* **193**, 28–51 (2017)
34. J. Ye, P.R. Medwell, E. Varea, B.B. Dally, H.G. Pitsch, An experimental study on MILD combustion of prevaporised liquid fuels. *Appl. Energy* **151**, 93–101 (2015)